AGU PUBLICATIONS

Space Weather

RESEARCH ARTICLE
10.1002/2013SW000994

Special Section:
The Crater Special Issue of Space Weather: Building the Observational Foundation to Deduce Biological Effects of Space Radiation

Key Points:
- Vavilov corrections should be incorporated into simulated results
- The predictions of the transport codes reasonably agree with the CRaTER LET
- The observed LET can be used to help validate space radiation transport codes

Correspondence to:
J. A. Porter,
jander40@utk.edu

Citation:
Porter, J. A., L. W. Townsend, H. Spence, M. Golightly, N. Schwadron, J. Kasper, A. W. Case, J. B. Blake, and C. Zeitlin (2014), Radiation environment at the Moon: Comparisons of transport code modeling and measurements from the CRaTER instrument, *Space Weather*, *12*, 329–336, doi:10.1002/2013SW000994.

Received 30 SEP 2013
Accepted 6 MAY 2014
Accepted article online 12 MAY 2014
Published online 2 JUN 2014

Radiation environment at the Moon: Comparisons of transport code modeling and measurements from the CRaTER instrument

Jamie A. Porter[1], Lawrence W. Townsend[1], Harlan Spence[2], Michael Golightly[2], Nathan Schwadron[2], Justin Kasper[3], Anthony W. Case[4], John B. Blake[5], and Cary Zeitlin[6]

[1]Department of Nuclear Engineering, University of Tennessee, Knoxville, Knoxville, Tennessee, USA, [2]Institute for the Study of Earth, Oceans, and Space, University of New Hampshire, Durham, New Hampshire, USA, [3]Department of Atmospheric, Oceanic and Space Sciences, University of Michigan, Ann Arbor, Michigan, USA, [4]High Energy Astrophysics Division, Harvard Smithsonian Center for Astrophysics, Cambridge, Massachusetts, USA, [5]Aerospace Corporation, El Segundo, California, USA, [6]Space and Engineering Division, Southwest Research Institute, Boulder, Colorado, USA

Abstract The Cosmic Ray Telescope for the Effects of Radiation (CRaTER), an instrument carried on the Lunar Reconnaissance Orbiter spacecraft, directly measures the energy depositions by solar and galactic cosmic radiations in its silicon wafer detectors. These energy depositions are converted to linear energy transfer (LET) spectra. High LET particles, which are mainly high-energy heavy ions found in the incident cosmic ray spectrum, or target fragments and recoils produced by protons and heavier ions, are of particular importance because of their potential to cause significant damage to human tissue and electronic components. Aside from providing LET data useful for space radiation risk analyses for lunar missions, the observed LET spectra can also be used to help validate space radiation transport codes, used for shielding design and risk assessment applications, which is a major thrust of this work. In this work the Monte Carlo transport code HETC-HEDS (High-Energy Transport Code-Human Exploration and Development in Space) is used to estimate LET contributions from the incident primary ions and their charged secondaries produced by nuclear collisions as they pass through the three pairs of silicon detectors. Also in this work, the contributions to the LET of the primary ions and their charged secondaries are analyzed and compared with estimates obtained using the deterministic space radiation code HZETRN 2010, developed at NASA Langley Research Center. LET estimates obtained from the two transport codes are compared with measurements of LET from the CRaTER instrument during the mission. Overall, a comparison of the LET predictions of the HETC-HEDS code to the predictions of the HZETRN code displays good agreement. The code predictions are also in good agreement with the CRaTER LET measurements above 15 keV/μm but differ from the measurements for smaller values of LET. A possible reason for this disagreement between measured and calculated spectra below 15 keV/μm is an inadequate representation of the light ion spectra in HETC-HEDS and HZETRN code calculations. It is also clear from the results of this work that Vavilov distributions need to be incorporated into the HETC-HJEDS code before it will be able to recreate the observed LET spectra measured by the CRaTER instrument.

1. Introduction

In June 2009, NASA launched the Lunar Reconnaissance Orbiter (LRO) spacecraft with four main objectives. One of these objectives is to characterize the lunar radiation environment for future manned missions. To accomplish this objective, the LRO carries the Cosmic Ray Telescope for the Effects of Radiation (CRaTER) instrument [*Spence et al.*, 2010]. The CRaTER telescope consists of three pairs of thin and thick silicon detectors separated by two segments of tissue equivalent plastic (TEP), all in an aluminum casing. In each silicon detector, energy deposition is measured and converted into linear energy transfer (LET). LET is a useful measurement because of its close relationship to biological effects from radiation exposure. The TEP segments represent self-shielding by body tissue.

HETC-HEDS (High-Energy Transport Code-Human Exploration and Development in Space), a three-dimensional Monte Carlo radiation transport code, is used to estimate the LET in each of CRaTER's components [*Townsend et al.*, 2005]. For comparison, estimates are also made using the HZETRN 2010 transport code. HZETRN (High *Z* and Energy Transport) is a one-dimensional, deterministic transport code, developed at NASA Langley Research Center, that is commonly used for estimating space radiation risk and shielding requirements [*Slaba et al.*, 2010].

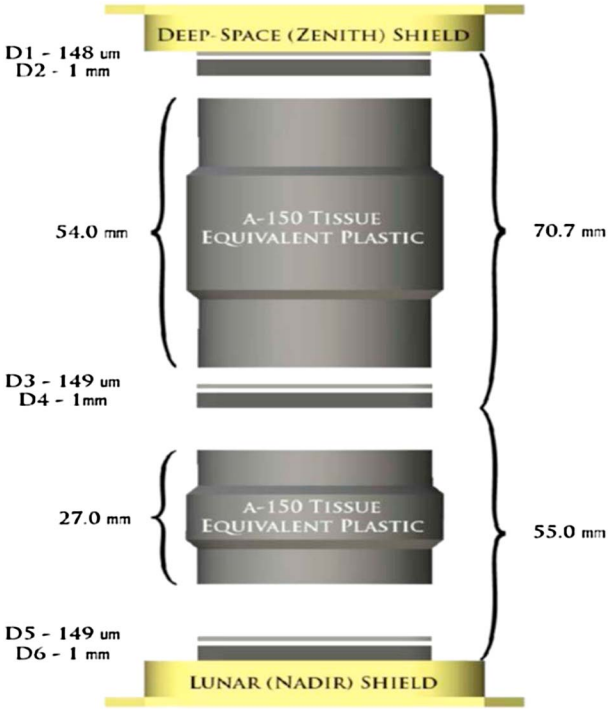

Figure 1. Instrument layout.

A major purpose of this analysis is to compare 1.5 years (29 June 2009 through 31 December 2010) of LRO experimental data and HETC-HEDS simulated data for particles that penetrate the complete length of the CRaTER detector. HETC-HEDS has been used previously to characterize the environment seen by CRaTER using different simulation methodologies [*Townsend et al*., 2009; *Farmer et al*., 2007; *Charara*, 2008; *Anderson and Townsend*, 2011a, 2011b]. Another purpose of the study is to investigate using the measured LET spectra from CRaTER as a validation tool for space radiation transport codes, such as the deterministic code HZETRN. The CRaTER LET data can serve to test the input particle flux data and the electromagnetic and nuclear interaction models/data used within the transport codes.

In this work, the energy losses of the primary and secondary ions that pass through the entire instrument starting at the zenith-pointing end are simulated using the HETC-HEDS Monte Carlo and HZETRN deterministic radiation transport codes then converted to LET and compared with measurements of LET in the D1/D2 silicon components of the CRaTER instrument. Differences in the measured values of LET and the calculated values from the transport codes, for minimum ionizing ions, will be discussed. The paper begins with a brief description of the CRaTER instrument configuration and operation. This is followed by a short discussion of the HETC-HEDS and HZETRN transport methods and collision models. Next, the computational methodology and results of the analyses are presented. The paper concludes with a summary of the main findings and suggestions for future work.

2. CRaTER

In order to safely return humans to the Moon for extended periods of time, the radiation environment of the Moon needs to be properly understood. The CRaTER instrument was designed to characterize the radiation environment and its biological impacts for extended or permanent manned missions. Since the exact track length of each charged particle through an individual detector is unknown, the energy deposition is divided by the most probable path length for an isotropic distribution of incident ions in order to obtain LET. For an isotropic distribution of incident particles within the instrument acceptance, this results in an average increase in track length of 1% of the Si detector thickness because the instrument design and triple-coincidence requirement restrict particles to within ±16.5° of normal incidence on the detector. Since the instrument measures energy deposited by charged particles and not their actual energy losses, this is not a true LET measurement. Nevertheless, for these simulations, it will be referred to as such, although the measurements are closer to lineal energy, which is the energy deposited per mean chord length [*International Commission on Radiation Units and Measurements*, 1993]. Radiation concerns, however, are not limited to primary particles only. While usually lower in LET, secondary radiation produced by nuclear interactions in the instrument may also enter the detection window causing the LET spectra to differ from that resulting from the primary only. The energy deposition from the observed CRaTER spectra include contributions from both primary particles and their interaction products and depend on numerous other factors including phase of the solar cycle, equipment orientation, etc. [*Vondrak et al*., 2010]. The LRO spacecraft provides some shadow shielding in the vicinity of the detector but has no significant effect on the particles that penetrate the entire instrument from one end to the other. An aluminum casing around CRaTER shields incoming particles with energies less than about 10 MeV. Figure 1 shows the dimensions and

configuration of the CRaTER sensor. Each CRaTER component is separated by a thin vacuum void, whose dimensions are not displayed in the figure. The aluminum caps on each end of the detector are ~0.8 mm (~0.22 g cm^{-2}) in thickness.

CRaTER has zenith (facing deep space) and nadir (facing Moon) ends, which are both penetrated by incoming particles. For the purpose of this analysis, it is assumed that all triple-coincidence particles enter from the zenith end. It is assumed that albedo particles are a negligible contribution to the triple-coincidence particles. Each detector pair consists of a thick (for low LET particles) and a thin (for high LET particles) silicon detector in order to cover the entire LET spectrum. Thin (0.034 g cm^{-2}) detectors (D1, D3, and D5) respond to energy deposits up to 300 MeV while thick (0.23 g cm^{-2}) detectors (D2, D4, and D6) saturate at 88 MeV. Sandwiched between the detector pairs are two tissue equivalent plastic (TEP) segments. The first TEP segment is 54 mm (6.086 g cm^{-2}) while the second is 27 mm (3.043 g cm^{-2}). TEP consists of a mixture of hydrogen, carbon, nitrogen, oxygen, fluorine, and calcium. TEP is used as a human tissue surrogate to determine effects of body self-shielding by human tissue overlaying the blood-forming organs [*Spence et al*., 2010]. Prior to launching LRO, CRaTER was calibrated using radioactive sources and a variety of charged particle beams at three different laboratories [*Spence et al*., 2010].

Particles penetrate CRaTER as follows: A charged particle with enough energy to pass through the first aluminum cap enters D1. By ionizing and exciting the Si atoms, the particle deposits energy in the detector. If nuclear interactions occur, secondary particles are produced, which also deposit energy. If a particle has sufficient energy, it can interact with the Si detectors deeper in the telescope stack. Those detectors that receive sufficient energy deposition will cross their trigger threshold. If any detector crosses its threshold, then a pulse height analysis (PHA) is conducted on each detector to measure the energy deposition. PHA converts pulse height to energy deposition using analog to digital converters to convert the energy deposited into an analog-digital number (ADU). If the particular detector coincidence is desirable, then the pulse heights for all six detectors are stored and telemetered. On the ground, each ADU value is then converted to energy deposited. Then, it is divided by the most probable track length to yield the measured LET [*Spence et al*., 2010].

3. HETC-HEDS

HETC-HEDS (High-Energy Transport Code-Human Exploration and Development in Space) is a three-dimensional Monte Carlo transport code that simulates particle cascades involving incident nucleons, light ions, heavy ions, and their secondaries produced by nuclear collisions. Primary and secondary particles' angles, energies, collisions, etc. are followed until the particle escapes the system, undergoes an interaction, decays, or comes to rest from energy lost. For each simulation, there is a geometry file that models the dimensions, densities, and materials for, in this case, CRaTER. An initial angle, energy, and particle type of the incoming ion is input by the user. Using this input data, HETC-HEDS simulates the track of the primary particle and all the subsequent secondaries produced through interaction with the target materials. A complete history file containing the data about each particle is produced. Neutrons produced below a user-specified cutoff energy and photons are not transported. For this study the neutron cutoff energy was set to 1 MeV. The neutron spectra are saved in an output file for possible transport using neutron transport codes such as Multigroup Oak Ridge Stochastic Experiment (MORSE) [*Emmett*, 1985] or Monte Carlo N-Particle (MCNP) [*X-5 Data Team*, 2003]. HETC-HEDS uses the continuous slowing down approximation, Bethe-Bloch theory [*Turner*, 2004], to treat excitation and ionization reactions for light and heavy ions, protons, charged pions, and muons [*Townsend et al*., 2005]. Breakup of heavy charged particles into lighter secondaries in nuclear collisions is modeled using a modified version of the NUCFRG2 semiempirical nuclear fragmentation code developed at NASA Langley [*Wilson et al*., 1994]. A more detailed explanation of HETC-HEDS inner workings and benchmarking is given in the following references: *Townsend et al*. [2005], *Miller and Townsend* [2004, 2005], *Charara et al*. [2008], and *Heinbockel et al*. [2011a, 2011b]. HETC-HEDS, however, does not follow the liberated electrons (delta rays) produced by Coulomb interactions. Thus, the code calculates energy lost using the difference between the particle energies entering and exiting a target component (true LET) but not the actual energy deposited.

4. HZETRN

HZETRN (high-charge-and-energy transport) simulates free-space radiation transport and shielding [*Wilson et al*., 1995]. HZETRN is based on a straight-ahead approximation to solve a one-dimensional formulation of

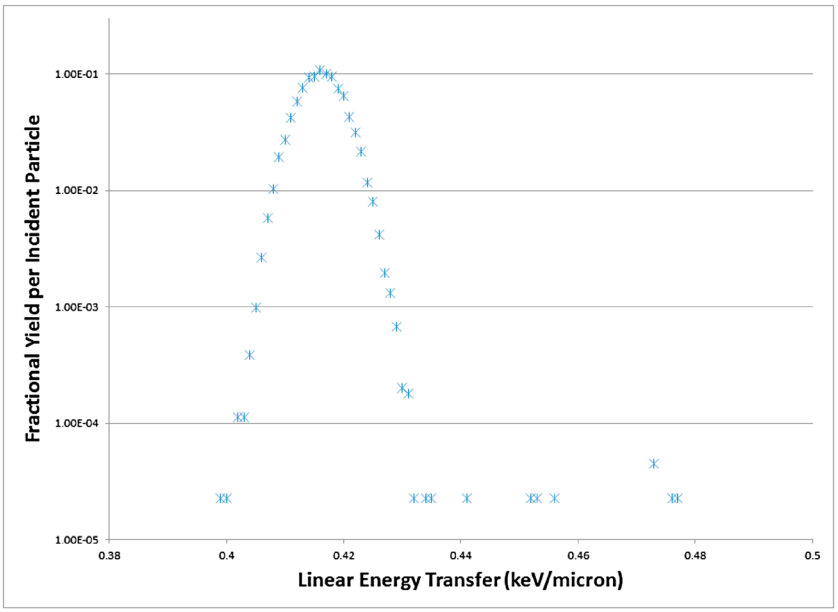

Figure 2. Distribution of LET values in D2 produced by 1000 MeV protons incident upon CRaTER, as modeled by HETC-HEDS.

the Boltzmann transport equation using a combination of analytical and numerical techniques. For simplification purposes, a continuous slowing down process is substituted for long-range Coulomb force and electron interactions, and Bethe's theory is used to calculate atomic stopping power coefficients for energies above a few MeV using a scaling approximation with proton stopping power. Further detail is discussed in *Wilson et al.* [1995]. As with HETC-HEDS, HZETRN does not follow the liberated delta rays. Instead, it also calculates true LET using the Bethe-Bloch formalism but not the actual energy deposited. The Ramsauer formalism determines total cross sections, and fits to quantum calculations give nuclear absorption cross sections. Nuclear fragmentation cross sections are calculated using semiempirical abrasion-ablation fragmentation model NUCFRG3 [*Adamczyk et al.*, 2012], an updated version of NUCFRG2 that incorporates an improved electromagnetic dissociation model and a coalescence model to describe light ion production processes. User input for HZETRN consists of shielding materials, shield thicknesses, and desired radiation environment. The output lists fluxes, doses, alternate risk estimates, and LET. The user enters in mass number, charge, and number density for each shielding material. Using these inputs, cross sections are produced for each material listed. Many widely researched radiation environments are already incorporated in HZETRN. If the environment does not already exist, the energy spectra for each ion are provided by the user. For a more detailed understanding of HZETRN inner workings and benchmarking, refer to *Wilson et al.* [1995] and *Slaba et al.* [2010].

5. Methodology

For the HETC-HEDS simulations, ions of all elements from protons to iron were used. Each ion was simulated using 100,000 particles for each energy increment as follows: 20–100 MeV/nucleon in increments of 5 MeV/nucleon, 100–200 MeV/nucleon in increments of 10 MeV/nucleon, 200–1000 MeV/nucleon in increments of 100 MeV/nucleon, and 1000–3000 MeV/nucleon in increments of 250 MeV/nucleon.

Energy loss values for each ion in each component are obtained by averaging over the particle histories for each particle type and incident energy increment.

This work assumes an isotropic distribution of incident angles in the zenith field of view. The zenith field of view of 16.5° gives the steepest angle that a particle can enter and still penetrate the entire detector stack. We concentrate only on particles that penetrate the entire detector stack (thereby causing a coincident event in D2, D4, and D6). For protons this requires energies greater than 120 MeV. See Figure 4 in *Case et al.* [2013] for the required energies for complete penetration of other species up to iron. The thick detectors are used to define the required coincidence because they have a lower energy deposition trigger than the thin detectors. This ensures that the full range of ions as light as protons are incorporated. Since the LET values above

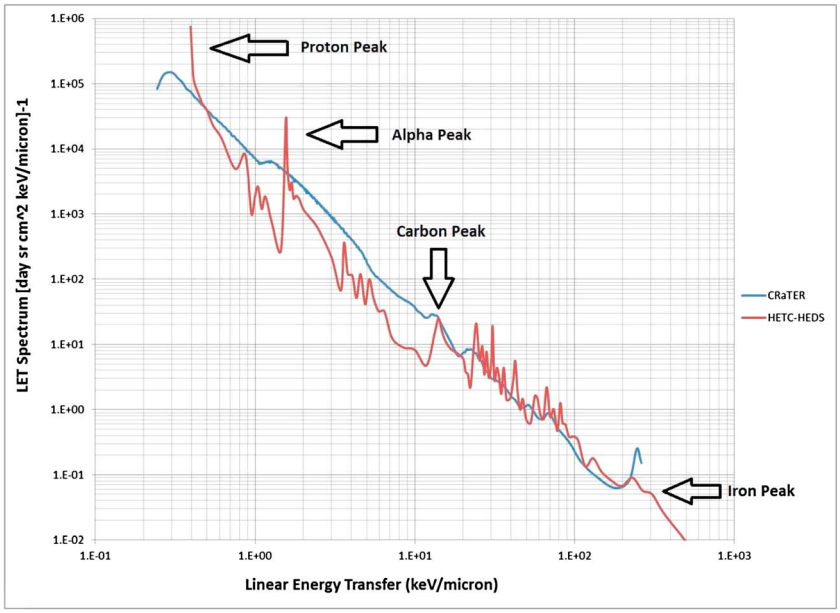

Figure 3. Linear energy transfer spectrum for observed CRaTER data and HETC-HEDS completely penetrating particles.

3000 MeV/nucleon are very close to those at 3000 MeV/nucleon, all incident particles with energies above 3000 MeV/nucleon are treated as 3000 MeV/nucleon incident particles and are added to the 3000 MeV/nucleon particle fluxes for transport.

Figure 2 shows a sample spectrum of LETs in D2 for incident protons at 1000 MeV. Similar spectra are generated for every ion species at all energy increments listed above. The width of the peak in the distribution of LET values is due to the effects of straggling. The tail LET values beyond ~ 0.44 keV/μm are the result of target fragments and recoils resulting from nuclear collisions. To generate a LET spectrum for comparison with the CRaTER LET measurements, the LET spectra generated by the HETC-HEDS simulations are folded with an input galactic cosmic rays (GCR) spectrum for the 29 June 2009 to 31 December 2010 time frame of the mission, obtained from the Badhwar O'Neill galactic cosmic ray environment model [*O'Neill*, 2010]. During this time period, no significant solar energetic particle events occurred so that the CRaTER observations can be compared directly to expectations from GCR models. The LET distribution spectrum in each silicon detector is then calculated for each particle that penetrated the entire detector stack.

In the present simulations, the peak locations for minimizing ionizing particles in the CRaTER data are clearly at lower values of the LET than those obtained with Bethe-Bloch theory [*Turner*, 2004]. From the work of *Bichsel* [1988], the discrepancies may be due to using the average energy loss in the calculation, whereas peaks in the data reflect the most probable energy loss. Actual energy loss distributions in thin detectors follow the Landau/Vavilov form, with a peak (most probable) value that is always smaller than the mean; the difference between the peak and the mean is a function of detector thickness. The effect is much less pronounced for heavy ions. On the other hand, it is very apparent for protons and ^{4}He, because of their lower, and widely separated, minimum-ionizing peak LET values. Hence, the calculations need to be corrected to account for this effect.

6. Results

The LET spectrum for these triple-coincidence particles from HETC-HEDS simulations and the triple detector coincidences for the observed CRaTER data [*Case et al.*, 2013] are plotted in Figure 3. For HETC-HEDS, the proton peak (leftmost peak in Figure 3) is at ~0.39 keV/μm. The minimizing ionizing value obtained from Bethe-Bloch theory is 0.37 keV/μm [*Wilson et al.*, 1991]. The observed CRaTER data have a proton peak located at ~0.3 keV/μm, which is lower than the theoretical Bethe-Bloch value. The HETC-HEDS ^{4}He peak is ~1.55 keV/μm (as obtained from Bethe-Bloch theory) while the observed data peak is ~1.2 keV/μm.

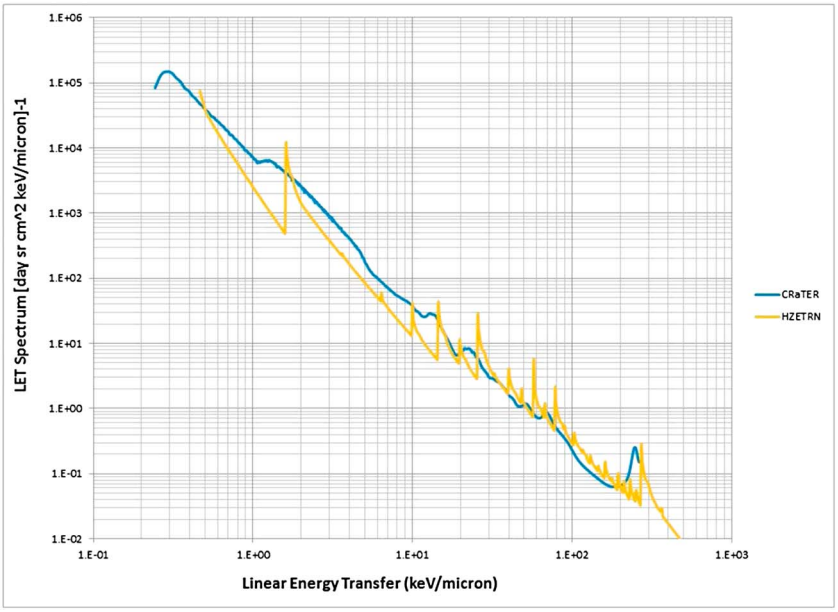

Figure 4. Linear energy transfer spectrum for observed CRaTER data and HZETRN 2010.

As discussed above, the most probable LET for high-energy ions is lower than the average LET [*Bichsel*, 1988]. Using a Vavilov distribution would shift each ion energy distribution. To quantify this idea, we calculated the most probable energy deposition values from a Vavilov distribution, rather than the average energy loss values used herein, for protons, ^{4}He, carbon, and iron ions at energies corresponding to their minimum ionizing peaks. For protons the minimum-ionizing peak shifts from 0.39 keV/μm to 0.3 keV/μm. For ^{4}He, the peak shifts from 1.55 keV/μm to 1.19 keV/μm. For carbon, the peak shifts from 15.2 to 12 keV/μm. For iron, the peak shift is from 306 to 245 keV/μm. These are in very good agreement with the values obtained from the CRaTER instrument (0.3, 1.2, 12.7, and 245 keV/μm for protons, ^{4}He, carbon, and iron, respectively). Fully implementing corrections based upon a Vavilov distribution is beyond the scope of the present work, since it involves corrections for every ion (primary and secondary), at every energy deposition value in the transported spectrum. These corrections will be fully implemented in future work.

From Figure 3, we note that the overall agreement between HETC-HEDS predictions and the CRaTER measurements for LET values above 15 keV/μm is reasonably good except for the minimum ionizing peaks being sharper for HETC-HEDS than for CRaTER. However, below 15 keV/μm, the CRaTER measurements are consistently higher in magnitude than the HETC-HEDS calculations, except for the very high, sharp peaks for minimum ionizing protons and ^{4}He displayed for HETC-HEDS. The LET range below 15 keV/μm corresponds to contributions from ions lighter than boron. The comparison suggests the possibility that the proton ^{2}H, ^{3}H, ^{3}He, and ^{4}He spectra produced by the code may be underestimated, when compared with the instrument data. Secondary light ion production in the HETC-HEDS event generator involves the use of a coalescence model to form light ions from secondary protons and neutrons produced in nuclear collisions. This issue will be investigated in future work by including a more sophisticated light ion coalescence model in the event generator [*PourArsalan and Townsend*, 2013]. The proton peak for the HETC-HEDS curve does not extend below the value for the minimum-ionizing LET due to the use of the Bethe-Bloch formalism in the simulation.

HZETRN 2010 was also used for simulations involving only those incident particles and energies that have the ability to penetrate the entire detector stack. The results are displayed in Figure 4. As was the case for the HETC-HEDS simulations displayed in Figure 3, the proton peak does not extend below the minimum ionizing LET value due to the use of the Bethe-Bloch formalism in a continuous slowing down approximation in the code calculations. The input GCR spectrum for these calculations is the same one used for the HETC-HEDS calculations presented herein. Other than for protons (first peak from the left) and ^{4}He particles (second peak from the left), the agreement between the data and calculations for the locations of the minimum ionizing peaks for heavier ion species ($Z > 2$) is good. As was the case for the HETC-HEDS results, the proton and ^{4}He minimum ionizing peak values are higher in LET than the observed CRaTER data. Again, this appears to be due to

Table 1. Total Flux and LET-Averaged Flux Versus LET Range for CRaTER, HETC-HEDS, and HZETRN

	Total Flux ([d sr cm^2]$^{-1}$)		
LET Range (keV/μm)	CRaTER	HETC-HEDS	HZETRN
0–15	4.147E + 04	2.859E + 04	1.105E + 04
15–500	2.725E + 02	2.479E + 02	2.312E + 02

the use of average energy depositions rather than most probable energy depositions in the HZETRN code. The observed data from CRaTER also have broader peaks than HZETRN because fluctuations in actual particle energy depositions are not accounted for in HZETRN, which analytically calculates stopping powers at the exit of each component as the particles traverse the centerline of the sensor stack. In addition, the HZETRN calculations, which are one-dimensional, assume that all particle trajectories are straight lines passing down the axis of the instrument from the zenith end through the nadir end. As was the case for the HETC-HEDS calculations, the LET spectra obtained with HZETRN 2010 are lower than the CRaTER measurements for LET values less than 15 keV/μm, except for the large proton and ^{4}He minimum ionizing peaks. These results suggest that the coalescence model used in HZETRN 2010 for light ion production also needs to be improved. Note, however, that these light ion discrepancies for HETC-HEDS and HZETRN 2010, which only involve $A = 2$ and $A = 3$ isotopes, are not a significant contributor to radiation risk from GCRs for astronauts since all hydrogen ($Z = 1$) and helium ($Z = 2$) isotopes only contribute ~10% of the dose equivalent [*Walker et al.*, 2013]. These HZETRN 2010 results also indicate that Vavilov distributions need to be incorporated into the code before it will be able to recreate the observed LET spectra measured by the CRaTER instrument. Such corrections are not presently part of the code package.

Table 1 displays comparisons of the total fluxes of particles within the 0–15 keV/μm and 15–500 keV/μm ranges for the CRaTER data and the current HETC-HEDS and HZETRN calculations. For the lower LET range, the HETC-HEDS calculations account for about 70% of the data. The HZETRN results are approximately 75% lower than the data. For the higher LET range, the HETC-HEDS results account for 91% of the CRaTER data, and the HZETRN results account for 85%. The large difference for HZETRN below 15 keV/μm may be due to the paucity of mass number 2 and 3 particles in the HZETRN spectrum and/or to the internal interpolation method (unknown to us) used to match the input GCR spectrum with the energy grid in the transport code.

Figure 5 compares HZETRN 2010 with HETC-HEDS simulations. The agreement between the HZETRN and HETC-HEDS prediction is fairly good, especially considering that HZETRN is a one-dimensional deterministic (analytical) transport code, whereas HETC-HEDS is a fully three-dimensional, Monte Carlo transport code.

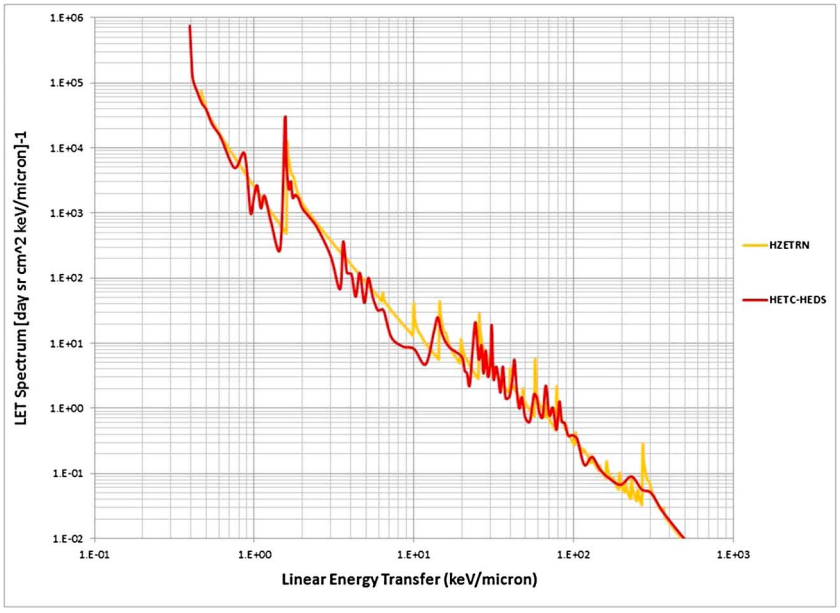

Figure 5. Predicted linear energy transfer spectra obtained from HETC-HEDS and HZETRN 2010 transport codes for the time period between 29 June 2009 and 31 December 2010.

The differences in the heights and widths of the minimum ionizing peaks are largely the result of differences between the point quantity analytical methods used in HZETRN and the finite difference methods used in HETC-HEDS to calculate LET values.

7. Conclusions

Presented in this work is a synopsis of the CRaTER instrument design and materials, the explanation and methodology of the HETC-HEDS Monte Carlo transport code, and HZETRN deterministic transport code. To illustrate the use of the CRaTER data for transport code validation, which was a major thrust of this work, comparisons of the observed CRaTER data, HETC-HEDS simulated data, and HZETRN results were made. There is fairly good agreement among all three spectra for LET values larger than 15 keV/μm. At lower LET values, both transport codes tend to underestimate the LET spectra suggesting that the light ion inputs and production in their input nuclear collision models may be underestimated and should be further investigated. It is also clear that Vavilov distributions need to be incorporated into the transport codes before they will be able to recreate the observed LET spectra measured by the CRaTER instrument. Incorporating Vavilov distributions into the HETC-HEDS code, because it is not a trivial undertaking, will be the subject of future work.

Acknowledgments
The CRaTER data for this paper are available for download at http://geo.pds.nasa.gov/missions/lro/. The HETC-HEDS and HZETRN data are available upon request from the first author. This work was supported at University of Tennessee under agreement 11-107 with the University of New Hampshire and at the University of New Hampshire under the NASA CRaTER contract NNG11PA03C. The authors wish to thank Joe Mazur of the Aerospace Corporation for his contributions to the early analytical phases of this work.

References

Adamczyk, A. M., R. B. Norman, S. I. Sriprisan, L. W. Townsend, J. W. Norbury, S. R. Blattnig, and T. C. Slaba (2012), NUCFRG3: Physics improvements to the nuclear fragmentation model, *Nucl. Instrum. Methods Phys. Res., Sect. A*, *678*, 21–32, doi:10.1016/j.nima.2012.02.021.

Anderson, J. A., and L. W. Townsend (2011a), LET comparisons for the CRaTER instrument on LRO and HETC-HEDS, 2011 IEEE Aerospace Conference, Big Sky, MT, March 5–12, 2011a.

Anderson, J. A., and L. W. Townsend (2011b), Dose estimates for the CRaTER instrument on LRO using HETC-HEDS, 56th Annual Meeting of Health Physics Society, West Palm Beach, FL, June 26–30, 2011b.

Bichsel, H. (1988), Straggling in thin silicon detectors, *Rev. Mod. Phys.*, *60*, 663–699, doi:10.1103/RevModPhys.60.663.

Case, A. W., J. C. Kasper, H. E. Spence, C. J. Zeitlin, M. D. Looper, M. J. Golightly, N. A. Schwadron, L. W. Townsend, J. E. Mazur, and J. B. Blake (2013), The deep-space galactic cosmic ray lineal energy spectrum at solar minimum, *Space Weather Int. J. Res. Appl.*, doi:10.1002/swe.20051.

Charara, Y. M. (2008), Characterization of the cosmic ray telescope for the effects, PhD Dissertation, Department of Nuclear Engineering, University of Tennessee, Knoxville.

Charara, Y. M., L. W. Townsend, T. A. Gabriel, C. J. Zeitlin, L. H. Heilbronn, and J. Miller (2008), HETC-HEDS code validation using laboratory beam energy loss spectra data, *IEEE Trans. Nucl. Sci.*, *55*, 3164–3168.

Emmett, M. B. (1985), MORSE-CGA: A Monte Carlo radiation transport code with array geometry capability, ORNL-6174 (April 1985).

Farmer, C. M., Y. M. Charara, and L. W. Townsend (2007), LET spectra of iron particles on A-150: Model predictions for the CRaTER detector, 37th International Conference on Environmental Systems (ICES), Chicago, IL, July 9–12, 2007. SAE Paper No. 2007-01-3113.

Heinbockel, J. H., et al. (2011a), Comparison of the transport codes HZETRN, HETC, and FLUKA for a solar particle event, *Adv. Space Res.*, *47*, 1079–1088.

Heinbockel, J. H., et al. (2011b), Comparison of the transport codes HZETRN, HETC, and FLUKA for galactic cosmic rays, *Adv. Space Res.*, *47*, 1089–1105.

International Commission on Radiation Units and Measurements (ICRU) (1993), International Commission on Radiation Units and Measurements, Quantities and Units in Radiation Protection Dosimetry, ICRU Report 51 (International Commission on Radiation Units and Measurements, Bethesda, MD).

Miller, T. M., and L. W. Townsend (2004), Double differential heavy ion production cross sections, *Radiat. Prot. Dosim.*, *110*, 53–60.

Miller, T. M., and L. W. Townsend (2005), Comprehensive cross section database development for generalized three dimensional radiation transport codes, *Nucl. Sci. Eng.*, *149*, 65–73.

O'Neill, P. M. (2010), Badhwar-O'Neill 2010 galactic cosmic ray flux model—Revised, *IEEE Trans. Nucl. Sci.*, *57*(6), 3148–3153, doi:10.1109/TNS.2010.2083688.

PourArsalan, M., and L. W. Townsend (2013), Emitted high energy light particle database development using a thermodynamic coalescence model, *J. Phys. Conf. Ser.*, *420*, 012063, doi:10.1088/1742-6596/420/1/012063.

Slaba, T. C., S. R. Blattnig, and F. F. Badavi (2010), Faster and more accurate transport procedures for HZETRN, *J. Comput. Phys.*, *229*(24), 9397–9417.

Spence, H. E., et al. (2010), CRaTER: The cosmic ray telescope for the effects of radiation experiment on the lunar reconnaissance orbiter mission, *Space Sci. Rev.*, *150*(1–4), 243–284, doi:10.1007/s11214-009-9584-8.

Townsend, L. W., T. M. Miller, and T. A. Gabriel (2005), HETC radiation transport code development for cosmic ray shielding applications in space, *Radiat. Prot. Dosim.*, *116*, 135–139.

Townsend, L. W., H. M. Moussa, and Y. M. Charara (2009), Monte Carlo simulations of energy losses by space protons in the CRaTER detector, *Acta Astronaut.*, doi:10.1016/j.actaastro.2009.08.007.

Turner, J. T. (2004), *Atoms, Radiation, and Radiation Protection*, 2nd ed., pp. 576, ISBN 0-471-59581-0, Wiley-VCH, Weinheim.

Vondrak, R. R., J. W. Keller, and C. T. Russell (Eds.) (2010), *Lunar Reconnaissance Orbiter Mission*, *Space Sci. Rev.*, vol. 150, Nos. 1–4, Springer, New York.

Walker, S. A., L. W. Townsend, and J. W. Norbury (2013), Heavy ion contributions to the organ dose equivalent for the 1977 galactic cosmic ray spectrum, *Adv. Space Res.*, *51*, 1792.

Wilson, J. W., L. W. Townsend, W. Schimmerling, J. E. Nealy, G. S. Khandelwal, F. A. Cucinotta, L. C. Simonsen, F. Khan, J. L. Shinn, and J. W. Norbury (1991), Transport methods and interactions for space radiations, NASA RP 1257, December 1991.

Wilson, J. W., J. L. Shinn, L. W. Townsend, R. K. Tripathi, F. F. Badavi, and S. Y. Chun (1994), NUCFRG2: A semiempirical nuclear fragmentation model, *Nucl. Instrum. Methods Phys. Res., Sect. B*, *94*, 95–102.

Wilson, J. W., F. F. Badavi, F. A. Cucinotta, J. L. Shinn, G. D. Badhwar, R. Silberberg, C. H. Tsao, L. W. Townsend, and R. K. Tripathi (1995), HZETRN: Description of a free-space ion and nucleon transport and shielding computer program, NASA TP 3495.

X-5 Data Team (2003), CCC-710/MCNP: Data libraries for MCNP, [file CCC-710_DATA.pdf].